



Published in final edited form as:

Dev Biol. 2008 January 1; 313(1): 359–370.

DISRUPTION OF THE PACAP GENE PROMOTES MEDULLOBLASTOMA IN PTC1 MUTANT MICE

Vincent Lelievre^{1,5,7}, Akop Seksenyan¹, Hiroko Nobuta¹, William H. Yong², Seririthanar Chhith¹, Pawel Niewiadomski, Joseph R. Cohen, Hongmei Dong¹, Avegail Flores¹, Linda M. Liao^{3,5}, Harley I. Kornblum^{1,4,5}, Matthew P. Scott⁵, and James A. Waschek^{1,5}

¹ Departments of Psychiatry and Biobehavioral Research/Mental Retardation Research Center, David Geffen School of Medicine, University of California at Los Angeles

² Department of Pathology and Laboratory Medicine, David Geffen School of Medicine, University of California at Los Angeles

³ Division of Neurosurgery, Department of Surgery, David Geffen School of Medicine, University of California at Los Angeles

⁴ Molecular and Medical Pharmacology, David Geffen School of Medicine, University of California at Los Angeles

⁵ Jonsson Comprehensive Cancer Center, David Geffen School of Medicine, University of California at Los Angeles

⁶ Departments of Developmental Biology and Genetics, Howard Hughes Medical Institute, Stanford University School of Medicine, Stanford, California, 94305

⁷ Inserm, U676, Hopital Robert Debre & Université Paris 7, IFR02, Paris, France

Abstract

Hedgehog (Hh) proteins and cAMP-dependent protein kinase A (PKA) generally play opposing roles in developmental patterning events. Humans and mice heterozygous for mutations in the Sonic hedgehog (Shh) receptor gene *patched-1* (*ptc1*) have an increased incidence of certain types of cancer, including medulloblastoma (MB), a highly aggressive tumor of the cerebellum. Despite the importance of PKA in Hh signaling, little is known about how PKA activity is regulated in the context of Hh signaling, or the consequences of improper regulation. One molecule that can influence PKA activity is pituitary adenylyl cyclase activating peptide (PACAP), which has been shown to regulate cerebellar granule precursor proliferation *in vitro*, a cell population thought to give rise to MB. To test for a PACAP/Hh interaction in the initiation or propagation of these tumors, we introduced a PACAP mutation into *ptc1* mutant mice. Deletion of a single copy of PACAP increased MB incidence approximate 2.5-fold, to 66%, thereby demonstrating that PACAP exerts a powerful inhibitory action on the induction, growth or survival of these tumors. Tumors from PACAP/*ptc1* mutant mice retained PACAP receptor gene expression, and exhibited superinduction of Hh target genes compared to those from *ptc1*^{+/-} mice. Moreover, PACAP inhibited proliferation of cell lines derived from tumors in a PKA-dependent manner, and inhibited expression of the Hh target gene *gli1*. The results provide genetic evidence that PACAP acts as a physiological factor that regulates the pathogenesis of Hh pathway-associated MB tumors.

Manuscript correspondence: James A. Waschek, Ph.D., 635 Charles E. Young Dr. South, University of California at Los Angeles, Los Angeles, CA 90095, Email: jwaschek@mednet.ucla.edu Tel: 310-825-0179; Fax 310-206-5061.

Publisher's Disclaimer: This is a PDF file of an unedited manuscript that has been accepted for publication. As a service to our customers we are providing this early version of the manuscript. The manuscript will undergo copyediting, typesetting, and review of the resulting proof before it is published in its final citable form. Please note that during the production process errors may be discovered which could affect the content, and all legal disclaimers that apply to the journal pertain.

INTRODUCTION

Studies in flies, fish, frogs, rodents and humans indicate that hedgehog (Hh) signaling is essential for the proper patterning and growth of many organ (Fukuda and Yasugi, 2002; Lum and Beachy, 2004; Poh et al., 2002) (for review). Cyclic AMP-dependent protein kinase A (PKA) opposes Hh action in many of these processes, causing the repression of Hh target genes until Hh signal relieves the repression. For example, loss of PKA in *Drosophila* mutants lacking Hh results in activation of Hh target genes and induction of patterning events that are normally dependent on Hh (Li et al., 1995). Conversely, overexpression of PKA counteracts the effects of Hh pathway activation (Li et al., 1995). PKA is believed to interfere with Hh action in *Drosophila* by phosphorylating and thereby priming the transcription factor cubitus interruptus (CI) for subsequent phosphorylation and processing into a repressor form (Aza-Blanc et al., 1997; Chen et al., 1999). On the other hand, PKA-dependent phosphorylation of Smo has been shown to promote the Hh pathway in *Drosophila* (Jia et al., 2004). Although the *Drosophila* PKA-phosphorylation sites on Smo are not conserved in vertebrates, studies in chicks indicate that PKA may have other Hh promoting actions in vertebrates (Tiecke et al., 2007). In any case, many aspects of the PKA antagonism of the Hh pathway are conserved in vertebrates. For example, overexpression of a dominant inhibitory form of PKA in the mouse neural tube mimicked overexpression of Shh (Epstein et al., 1996), and conversely, expression of a constitutively active form of PKA in zebrafish blocked the effects of Shh overexpression (Hammerschmidt et al., 1996). However the mechanisms that regulate PKA activity so that Hh signal transduction is kept at proper levels remain largely unknown in flies and vertebrates.

Mutations resulting in loss of function of human Shh elicit severe abnormalities of the developing brain, a condition called holoprosencephaly. Conversely, mutations that cause derepression of Shh target genes are associated with multiple cancer types including basal cell nevus syndrome (also called Gorlin syndrome) as well as MB. Such mutations have arisen in genes encoding the Shh receptor/tumor suppressor Patched-1 (Ptc1), the signal-transducing transmembrane protein Smoothed (Smo), and the downstream intracellular signaling protein Suppressor of fused (SuFu).

MB is the most common pediatric brain tumor and its recurrence is nearly always fatal. An understanding of the pathogenesis and growth regulatory mechanisms of this tumor is greatly needed, as is the development and optimization of appropriate animal models. Mice with targeted deletions of the *ptc1* gene are an excellent model for studying Hh pathway-associated pathology. *ptc1* mutant mice die on about embryonic day 9–10.5 due to multiple defects, including massive neural tube overgrowth (Goodrich et al., 1997). Heterozygous animals, however, develop relatively normally *in utero*, but have a significant incidence of a specific panel of tumors including MB, a phenotype similar to that of humans with hereditary *ptc1* mutations (Gorlin's syndrome).

PKA activity is regulated by a number of different mechanisms (Baillie et al., 2005), any of which might impinge on Hh signal transduction. In order to understand better how PKA might influence cerebellum tumorigenesis, we have begun to examine the possible role of a small peptide, pituitary adenylyl cyclase activating peptide (PACAP), that is known to regulate PKA in tissues expressing its receptor. We recently demonstrated in rodents that mRNAs for the PACAP receptor PAC1 and the Shh receptor Ptc1 are colocalized in the embryonic hindbrain ventricular zone (VZ), and in the postnatal external granule layer (EGL) of the cerebellum (Nicot et al., 2002; Waschek et al., 1998). These are the two germinal centers thought to give rise to MB in humans. PACAP has putative growth factor-like actions (Vaudry et al., 2000; Waschek, 2002) (for review) and is potentially supplied to cells in these centers by post-mitotic neurons in the developing hindbrain (Vaudry et al., 2000) and Purkinje cells in the developing

cerebellum (Nielsen et al., 1998). We showed that PACAP inhibits the expression of Shh target genes in embryonic hindbrain cultures (Waschek et al., 1998) and counteracts the proliferative actions of Shh in neuronal precursor cultures derived from the EGL (Nicot et al., 2002). These data set the stage for investigating whether loss of PACAP might affect the incidence and/or growth rate of MB tumors in *ptc1*^{+/-} mice. Here we investigated the incidence, onset, and gene expression patterns in MB tumors in *ptc1*^{+/-} that have a targeted deletion in the PACAP gene.

MATERIALS AND METHODS

Mouse housing conditions

Mice were housed according UCLA Institutional Guidelines including standard light-dark cycles with food and water ad libitum. All mice were daily monitored for signs of illness or tumor effects.

PACAP and *ptc1* mutant mice

The generation of mice with targeted mutations in the PACAP and *ptc1* genes were previously described (Colwell et al., 2004; Goodrich et al., 1997). All animals used in the present study were backcrossed for at least six generations to a C57BL/6J genetic background. *Ptc1* heterozygous (Hz) mice were initially bred with PACAP Hz or PACAP null mice to generate *ptc1* and *ptc1*/PACAP double heterozygous (DH) mutants. Mice used for the analyses were generated by interbreeding these DH mice or by breeding either *ptc1*^{+/-} or DH male mice with female PACAP^{+/-} mice. Genotyping by PCR (Colwell et al., 2004; Goodrich et al., 1997) was performed at six week of age.

MB assessment

Mice were monitored daily for clinical signs of MB, such as lethargy, ataxia, balance defects, dehydration, and reduced grooming. When animals exhibited clinical signs, food (pellets and apple) was directly provided to animals to extend life span. When unable to take food, animals were sacrificed and autopsied. If presence of MB was confirmed, time of sacrifice was considered equivalent to date of death. The mean date of incidence was calculated using a non-linear regression analysis (sigmoid curve with variable slope) and performed using Graphprizm 4TM software.

Charaterization of tumors

Tumors collected from ten *ptc*^{+/-} and ten DH mice were fixed in 4% paraformaldehyde, paraffin-embedded, and sectioned at 6µm. Sections were deparaffinized in two xylene baths and rehydrated in decreasing concentrations of alcohol baths. A standard hematoxylin and eosin staining was conducted on some of these sections. For immunohistochemistry, antigens were retrieved by boiling the sections in solution containing 0.8mM citric acid and 7mM sodium citrate, adjusted pH 6.0 for 20 min and cooling for additional 20 min. Following endogenous peroxidase inactivation with 3% hydrogen peroxide solution for 10 min, sections were rinsed in PBS and blocked in PBS containing 5% normal goat serum. Primary antibody against synaptophysin (Santa Cruz, polyclonal, dilution 1:100) and GFAP (Neo Markers, polyclonal, dilution 1:200) were diluted in the blocking solution and incubated overnight at 4° C. After washes in PBS, biotinylated anti-rabbit secondary antibody (Vector) was diluted in PBS (1:200) and incubated for 30 min at room temperature. After additional washes in PBS, slides were incubated in avidin-biotin peroxidase solution (Vectastain ABC kit, Vector) for 30 min at room temperature. Sections were visualized using DAB substrate solution prepared from liquid DAB kit (Biogenex). Sections were then counterstained with DAPI for nuclear

visualization, washed in water, dehydrated in increasing concentrations of alcohol baths, xylene treated and coverslipped.

Ectopic cerebellar lesions

Postnatal day 28 mice were transcardially perfused with 4% paraformaldehyde. Brains were postfixed in 4% paraformaldehyde for 2 hr, cryoprotected, and sectioned at 12 μ m. After blocking, immunohistochemistry was performed with a Ki-67 (Vector, polyclonal, dilution 1:250) incubated for 1hr at 37°C. Following washes, secondary antibody (Cy3-conjugated anti rabbit, Jackson Immuno Research) was incubated for 45 min at room temperature. After additional washes, sections were coverslipped with Vectashield Mounting Media (Vector) containing DAPI for nuclear visualization. For In situ hybridization for PAC1 gene expression was carried out with ³³P as described (Waschek et al., 1998).

Isolation of MB cell lines

In a subset of animals showing clinical signs for MB, cerebella were dissected under strict aseptic conditions. Tumors were carefully separated from normal cerebellar tissue. Half of the tumor was quickly homogenized in guanidium isothiocyanate solution (GnTC) solution prior to RNA isolation. The second half was dissociated in trypsin/EDTA solution for 10 min. Trypsin was then inactivated by addition of several volumes of DMEM culture medium containing 20% inactivated fetal bovine serum (FBS). After centrifugation, the cell suspension was placed into a tissue culture flask in DMEM medium supplemented with 10% inactivated fetal bovine serum (FBS). Cultures were kept at 37°C in 5% CO₂ controlled atmosphere. Medium was replaced every week, until growing cell clusters appeared. Growing cells were expanded and grown in monolayer conditions, and passaged a few times prior to freeze in liquid nitrogen.

Isolation of granular cell progenitors (GC)

Cerebella were carefully and aseptically dissected from WT mice. GC isolation was performed using a Percoll gradient as previously described (Tao et al., 1997). Cells were cultured for 3 hours to allow contaminating cells to attach. GC were then removed using gentle pipetting and subjected to RNA extraction as described (Chomczynski and Sacchi, 1987).

Drugs

PACAP-38, forskolin, and H89 were obtained from Calbiochem.

β -galactosidase staining

Cells were fixed in 0.2% glutaraldehyde for 5 min, washed in PBS, then incubated overnight at 37°C in Xgal buffer (5-bromo-4-chloro-3-indolyl- β -D-galactopyranoside (Xgal) at a final concentration of 0.4 mg/ml (made from a 40 mg/ml stock in dimethylformamide), with 4 mM K₃Fe(CN)₆, 4 mM K₄Fe(CN)₆·6H₂O, 2 mM MgCl₂ in PBS.

Cyclic AMP assay

A commercial radioimmunoassay kit from Amersham used. Dissociated cells were seeded in 24-well tissue culture plates at the initial density of 50,000 cells/well. 48 hours later, culture medium was replaced by 460ul of serum-free medium containing 1mM of IBMX (Sigma). Twenty minutes later, 40 ul of peptides (100X), vehicle (DMSO) or drug (forskolin, 100X) were added for another 20 min. Culture medium was promptly removed by aspiration and wells rinsed once with 1ml of cold PBS, prior to cell extraction with 500ul of 6% TCA after a 10s sonication. Extracts were transferred into 1.5ml eppendorf tubes and frozen at -80C for 24hours. Samples were finally dried out in a speedvac apparatus and pellets reconstituted in

500ul of 0.05M acetate buffer. Diluted samples were analyzed for cAMP contents according to the manufacturer's protocol (Amersham) and cAMP quantified using a cAMP standard curve performed concomitantly.

PKA assay

MB57 cells were plated at a density of 15000 cells/cm² and left in culture for 48 hours in DMEM media containing penicillin/streptomycin/glutamine and 10% FBS. They were switched to media containing 1% serum 2h before the start of the experiment. The cells were incubated for 1h with H89 (3 μM) or DMSO as a control, and then forskolin (20 μM) or DMSO was added for another 1h. The cells were washed in PBS, harvested by scraping off, and flash frozen in liquid nitrogen. The cells were lysed in the NP-40 lysis buffer containing protease and phosphatase inhibitors for 30 minutes on ice, and then debris was removed by centrifugation. The protein extracts were subjected to PAGE on 7% polyacrylamide gels, and following transfer to PVDF membrane, to Western Blotting using the following primary antibodies: rabbit anti-phospho-PKA substrate (Cell Signaling; 1:5000), mouse anti-GAPDH (Imgenex; 1:2500).

Proliferation studies

In vitro thymidine incorporation on MB cells in culture was performed using the trichloroacetic acid (TCA) precipitation method. Dissociated tumor cells were seeded in 24-well tissue culture plates at the initial density of 50,000 cells/well and cultured in DMEM medium supplemented with 2% of heat-inactivated FCS (GibcoBrl/lifetechnology) and a cocktail of penicillin/streptomycin antibiotics. 48 hours later, medium was replaced with fresh medium for 2 hours prior to cell treatments with peptides and/or drugs for 6 hours. Drug treatments (5ul/500ul total volume) were performed using extemporaneously prepared 100X stock solutions. Thirty minutes later, ³H-thymidine (NEN/Perkinelmer), 1uCi/well, was then added. Cells were harvested 8 hours later. Cell cultures were washed with 500ul/well of PBS then lysed in 500ul of NAOH 0.5M. Cell extracts were transferred into 2-ml eppendorf tubes and supplemented with 500 ul of cold 20% TCA. DNA precipitation was allowed for 20 min on ice then samples were centrifuged at 20,000g, for 20 min at 4C. Supernatants were aspirated and the DNA-containing pellets washed with 500ul of 10% TCA. After a 10 min centrifugation, pellets were finally reconstituted in 500ul of 0.1M NAOH and transferred into scintillation vials while incorporated radioactivity was counted on a scintillation counter (Beckman) using 5ml of Aquasafe™ scintillation cocktail (Wallac). Cell proliferation by direct cell counting in other experiments was performed as previously described (Lelievre et al., 2000) with MB cells seeded at the initial density of 5,000 cells/ml into 24-well tissue culture dishes and grown in DMEM medium supplemented with 1% FCS (Invitrogen). After 24 h, PACAP or vehicle was added daily at a final concentration of 10nM, an equivalent amount of vehicle was added to control wells.

Competitive RT-PCR

The PAC₁ primer set was similar to the one used in a previous study (Nicot et al., 2002): sense primer, GGATGCTGGGATATGAATGACAG CACAGC, which recognized the sequences 1035–1064 of the mouse cDNA (D82935) and reverse primer, CCTTCCAGCTCCTCCATTTCTCT, which recognized the sequences 1495–1472 and 1466–1452 of the same cDNAs. This target sequence was chosen because it may contain additional cassettes corresponding to previously reported splice variants (Spengler et al., 1993). To quantify gene expression between samples, we included a set of 18S primers/competimer from Ambion. To ensure linear amplification for all the genes throughout the PCR cycles, a 1:7 ratio of 18S primer/competimer was determined. PCR was run for 35 cycles using 3step-procedure (30s denaturation at 96°C, 40s annealing at 58°C and finally a 40s extension at 72°C). Samples were run on Nu-sieve 3% agarose gels. Gel pictures were shot using a

Geldoc™ imaging system from Bio-Rad. Specificities of the different PCR amplifications were ultimately confirmed by sequencing.

Real-time RT-PCR

mRNAs encoding the genes of interest were first analyzed for secondary structure using M-fold software. Portions of sequences lacking significant secondary structure were imported into oligo6 software to design highly-stringent primer sets. Ultimately, these primers were blasted in cDNA databases to ensure their specificity. For *gli1*, we chose the following oligonucleotides: 5'-ATCTCTCTTTCTCCTCCTCC-3'OH and 5'-CGAGCCTGGCATCAGAA-3'OH, as sense and antisense primers, respectively. PCR amplification resulted in the specific formation of a 95bp sequence corresponding to the region 356–449 of the previously published sequence of mouse *gli1* mRNA (NM010296). For *gli3*, 5'-GATCCATCTCCTATTCCTCCA-3'OH and 5'-GATCCTAATGAAGGG CAAGTC-3'OH were used. The amplified 83 bp sequence corresponded to the 616–699 region of the published MN008130 sequence. For *Bmi1*, the following primer set 5'-TGTGTGGAGGGTACTTCATT-3'OH and 5'-AGGACAATACTTGCTGGTCTC-3'OH was used. This amplified a unique PCR fragment of 100 bp corresponding to the portion 383–486 of the published *Bmi1* gene (MUSBMI1B). For the mouse homologue of the *Mushashi* (*Msh1*) gene (NM_008629), 5'-TCAAGCTGCCAGAAGATGCTC-3'OH and 5'-GGAGAAGCGGGGACT CTGC-3'OH were used to specifically amplify a 84 pb sequence located in position (494–579). For *N-myc*, 5'-GGATGATCTGCAAGAACCCAG-3OH and 5'-GTCATCTTCGTCCGGG TAGAA-3OH primer set selectively amplified a unique 70pb band corresponding to the region 72–172 of the published *N-myc* sequence (M36277, whereas the following primer set 5'-ATCTACATCAACGCTCTGTGC-3OH and 5'-AAGGTGATGGTGGTCATTTTT-3OH spanned a 99pb amplicon of the region 801–899 of the granule cell progenitor marker *Math1* gene (D43694). To standardize the experiments we designed, using the same approach a primer set for the mouse β 2-microglobulin (β 2MG) gene (5-CCGGCTTGATGCTATC-3'OH and 5-AGTTCATGTTCGGCTTC-3'OH, as sense and anti-sense respectively) and another set for glyceraldehyde-3-phosphate dehydrogenase (*GAPDH*: 5'-GGCCTTCCGTGTTCTAC-3'OH and 5'-TGTCATCATACTTGGCAGGTT-3'OH). These oligonucleotides amplified an 87pb region encoding the nucleotides 99–185 of the published sequence (MM2BMR) and an 80pb piece spanning the area 1093–1173 of published *GAPDH* (XM111622) mRNA, respectively. Real time PCR was set up using sybergreen-containing supermix from Biorad, for 50 cycles of a 3-step procedure including a 20s denaturation at 96°C, a 15s annealing at 60–62°C, followed by a 20s extension at 72°C. Amplification specificity was assessed by melting curve and sequencing analyses. Quantification of each PCR samples was made using standard curves made from serial dilutions of control samples or of the corresponding cDNA cloned into PCRII vector. Differences between samples were calculated as the difference between the specific ratios (gene/ β 2MG or gene/*GAPDH*) calculated for each individual sample. As in competitive RT-PCR, specificities of the different PCR amplifications were ultimately confirmed by sequencing.

RESULTS

Generation of *ptc1+/-* PACAP +/- double mutants (DH) and assessment of Shh pathway activity in the cerebellum

We generated PACAP knockout (KO) mice on a C57BL/6J background, and confirmed loss of PACAP production by radioimmunoassay (Colwell et al., 2004). Consistent with that observed with other PACAP KO strains (Gray et al., 2001; Hashimoto et al., 2001), significant numbers of PACAP KO mice die before genotyping. However, heterozygous and surviving PACAP *-/-* mice show no subsequent increased morbidity under normal housing conditions.

We bred backcrossed PACAP KO males with C57BL/6-backcrossed *ptc1*^{+/-} females (Goodrich et al., 1997) to generate the first generation of DH mutants. These animals were fertile and were subsequently interbred to generate the animals used in the present study. Litters of DH x DH breedings were genotyped at six weeks of age to determine the survival of the various genotypes (Table 1). No *ptc1*^{-/-} and few PACAP^{-/-} mice were present at the time of genotyping among 130 offspring obtained from 26 matings.

To determine if the relative loss of PACAP in PACAP^{+/-} mice resulted in increased Hh pathway activity in the cerebella of asymptomatic *ptc1*^{+/-} mice, we determined the expression levels of the Shh target gene *gli1* in the cerebella of asymptomatic *ptc1*^{+/-} and DH mice at 1 and 6-month of age. We found that *gli1* mRNA levels were significantly increased in the cerebella of 1- and 6 month-old asymptomatic *ptc1*^{+/-} compared to wild-type mice, and increased even further in PACAP/*ptc1* double heterozygous (DH) mice (Fig. 1A). However, the levels of *gli1* gene expression in PACAP mutants (HZ or null) with both *ptc1* alleles intact were not elevated over that of wild type control mice (Fig. 1B). Reciprocally, levels of PACAP gene expression were not affected by monoallelic loss of *ptc1*, but were reduced, as expected, in PACAP^{+/-} and DH mice (Fig. 1C). These data suggest that Ptc1 and PACAP mutually inhibit Shh pathway activity in asymptomatic animals

MB induction and cancer survival

To determine whether the incidence of MB tumors increases in *ptc1*^{+/-} mice that also lack a PACAP allele, the incidence of MB over a one-year period was determined in mice derived from DH x DH matings and from matings of PACAP^{+/-} females with either *ptc1*^{+/-} or DH males. A total of 77 *ptc1* heterozygotes and 73 *ptc1*/PACAP DH mutants were analyzed. Mice were monitored on a daily basis, and the dates of death or appearance of neurological symptoms and subsequent sacrifice were recorded. The presence or lack of MB was determined by autopsy. Deletion of a single copy of the PACAP gene strongly enhanced MB frequency in *ptc1* mutants (Fig. 2A). Indeed, a 66% rate of MB was observed in DH mice, reflecting a 2.5-fold increased incidence compared to *ptc1*^{+/-} mice. The onset of clinical signs of MB (lethargy, ataxia, etc.) was also shifted to an earlier stage in DH mice (Fig. 2B). The mean date of occurrence of symptoms was 6.2 months in *ptc1*^{+/-} control mutants, similar to that reported by others (Goodrich et al., 1997; Wetmore et al., 2000). The mean date of occurrence in DH mutants was 4.8 months, six weeks sooner than in *ptc1* mutants. The incidences were maintained when the data were segregated on the bases of parental breeding (not shown).

The incidence of rhabdomyosarcoma in both groups was small, as previously shown in mice with this *ptc1*^{+/-} mutation (Goodrich et al., 1997; Wetmore et al., 2000). Out of more than 200 PACAP^{-/-} mice generated in our colony for other studies, none developed MB, indicating that complete loss of PACAP is insufficient to induce this tumor.

Characterization of MB tumors in DH mice

To characterize the MB tumors in DH mice, we dissected, formalin fixed, and paraffin-embedded ten tumors each from *ptc1*^{+/-} and DH mice. Similar to that reported in tumors from *ptc1*^{+/-} mice and from humans, tumors in DH mice were comprised of densely packed cells with pleomorphic, hyperchromatic carrot-shaped nuclei and with scant cytoplasm (Goodrich et al., 1997; Wetmore et al., 2000) (Fig. 3, top panel). Mitotic activity and occasional confluent areas of apoptosis were noted. By the criteria of Eberhart and colleagues, these tumors may be representative of moderately anaplastic human medulloblastomas (Berman et al., 2002). Tumors from either genotype lacked obvious nodularity (WHO schema (Kleihues et al., 1998)), similar that reported in *ptc1*^{+/-} tumors by others (Corcoran and Scott, 2001; Goodrich et al., 1997; Kimura et al., 2003; Wetmore et al., 2000). Also similar to tumors from *ptc1* mutant mice (Wetmore et al., 2000) and human MB (Ellison, 2002), immunocytochemistry on DH

tumors revealed varying degrees of synaptophysin and GFAP immunoreactivity (Fig. 3, bottom panels). In general, the staining for synaptophysin is extensive while the GFAP-positive cells are few and may represent reactive astrocytes. Analysis of tumors from 10 *ptc1*^{+/-} and 10 DH mice revealed no obvious differences in histological features on H&E staining or in patterns of synaptophysin or GFAP immunoreactivities.

PACAP receptor gene expression in hyperplastic regions of the EGL and MB tumors

We previously showed by *in situ* hybridization that mRNA for the PACAP-specific receptor PAC1 co-localized with that of *ptc1* in the postnatal cerebellar EGL as well as in the embryonic hindbrain ventricular zone. Given that one or both of these germinal zones are felt to give rise to MB, we were interested to know if PAC1 gene expression was present in MB tumors that presented in these mice. RT-PCR analysis of eight tumors indicated that the PAC1 gene was expressed in all tumors Fig. 4A. Moreover, *in situ* hybridization showed that PAC1 gene expression was present in patches of hyperplastic EGL at postnatal day 28 (Fig. 4B and C). These patches have been shown by others to persist in most *ptc1*^{+/-} animals for a few weeks after the EGL normally recedes, and have been proposed to represent premalignant lesions. Thus, PAC1 gene expression is present in granule precursors at an early stage and appears to persist in these cells as they develop into full tumors.

Expression of Hh target and other genes in MB samples

Our original hypothesis was that PACAP limits the activity of Shh in cerebellar precursors, and that loss of this inhibitory action might lead to higher hedgehog activity during the inductive and/or growth rate of these tumors. Shh pathway activity can be estimated by measuring the level of expression of Hh target genes. To determine if MB tumors in PACAP^{+/-} mice were associated with derepression of Shh pathway activity compared to those from *ptc1*^{+/-} mice, we compared the expression of Shh target genes from these groups of mice by real time RT-PCR. These studies revealed that the expression of three Shh target genes, *gli1*, *N-Myc* and *Bmi1*, was 2 to 5-fold higher in tumors from DH mice than in tumors from *ptc1*^{+/-} mice ($p < 0.01$), and higher than in normal cerebellum (CB) and freshly-isolated granular cell progenitors (GC) (Fig. 5), whereas *gli3* gene expression did not significantly differ in the two sets of tumors. Furthermore, gene expression in tumors from DH vs. *ptc1*^{+/-} mice was also increased for the Notch facilitator MSH1 ($p < 0.01$), which is overexpressed in human MB tumors. The fact that the Shh target genes *gli1*, *N-myc* and *Bmi1* were expressed at higher levels in tumors from DH mutants than in those from *ptc1*^{+/-} mice suggests that the reduction of PACAP in double-mutant mice promotes Shh pathway activity in tumors, or that a lack of PACAP during their formation results in tumors with higher Shh activity.

Effects of PACAP on proliferation and gene expression in primary medulloblastoma cell lines

To determine if PACAP signaling remained intact in MB tumors, we established primary cell lines from six different tumors. Like the intact tumors (Fig. 4A), these cell lines expressed transcripts for the PAC1 receptor (data not shown). All but one cell line responded to 10 nM PACAP with a significant reduction in DNA synthesis over an 8 hour treatment period (Table 2). One of these cell lines (#57) was selected for further studies. PACAP potently and dose-dependently stimulated cAMP production in these cells (Fig. 5A), indicating that these cells expressed receptors that were functional coupled to cAMP production. PACAP also dose dependently inhibited DNA synthesis in these cells in a manner that was fully blocked by 3 μ M of the PKA antagonist H89 (Fig. 5B). This concentration of H89 was selected as the minimal dose which blocked the effect of forskolin on PKA activity in these cells (data not shown). PACAP inhibition on cell proliferation remained effective over a 3-week period of time when 10nM PACAP were added daily (Fig. 5C). In addition to the antiproliferative action, PACAP inhibited gene expression for *gli1*, and reduced mRNA levels of math-1, a marker for

undifferentiated granule cell precursors (Fig. 5D). The effects on gene expression were mimicked the cAMP-inducing agent forskolin. These studies suggest that MB tumors in these mice retain the ability to respond to PACAP, and that the PACAP/PKA pathway might have utility as a therapeutic target for MB tumors with elevated Hh activity.

DISCUSSION

We describe here a new genetically-engineered spontaneous brain tumor model which combines a HH pathway mutation (*ptc1*) with a PACAP gene mutation. A novel aspect of the model created and tested here is that it addresses the biology and pathogenesis of MB tumors in the context of their development and known signal transduction pathways. The receptor for PACAP is expressed along with the HH receptor in the germinal center of the brain that gives rise to these tumors. PACAP acts in these germinal cells by increasing cAMP and activating protein kinase A (PKA). Studies that began in *Drosophila* and were extended to vertebrates had indicated that protein kinase A (PKA) antagonizes HH signaling at the level of signaling intermediates. However, the importance of this interaction in human disease models has never been demonstrated. Our hypothesis in deleting the PACAP gene from *ptc1* mutant mice was that removal of this potential inhibitory influence on HH pathway activity would cause an even higher and more rapid incidence of medulloblastoma. The findings of increased incidence and more rapid onset of tumors imply that secondary or concomitant genetic events leading to suppression of PKA activity may play a key role in transformation of neoplastic granular progenitor cells into medulloblastoma and perhaps in the induction of other tumors associated with overactive HH signaling.

To further reinforce our hypothesis that loss of PACAP would enhance activation of Shh pathway in tumors, we performed a set of gene expression analyses in tumors by real time RT-PCR. This analysis revealed that the expression of three Shh target genes, *gli1*, *N-Myc* and *Bmi1*, were increased 2 to 5-fold in tumors from DH mice compared to those from *ptc1*^{+/-} mice, whereas *Gli3* gene expression did not significantly differ. Previous studies reported that the former genes are induced by Shh in cerebellar granule precursor cells (Kenney et al., 2003; Leung et al., 2004; Wechsler-Reya and Scott, 1999), and overexpressed in human MB (Leung et al., 2004; Reifenberger et al., 1998; Yokota et al., 2004). Furthermore, recent studies have shown the important role of Gli1 in MB formation (Kimura et al., 2005). Gene expression of the Notch facilitator MSH1 (Yokota et al., 2004), which is also overexpressed in human MB, was increased in tumors from DH mice. Our results clearly demonstrated that the Shh target genes as well as MB markers (*gli1*, *N-myc* and *Bmi1*) were expressed at higher levels in tumors from DH mutants than in those from *ptc1*^{+/-} mice. This suggests that the reduction of PACAP in double-mutant mice maintains Shh pathway activity in tumors at a high level, or that a lack of PACAP during their formation results in tumors with higher Shh activity.

Because all tumors tested exhibited PAC1 receptor gene expression (Fig. 4A), as did all derived cell lines (data not shown), we tested the ability of the latter to respond to PACAP. All cell lines exhibited significant growth rate reduction when treated with PACAP (Table 2). The ability of PACAP to stimulate cAMP production was confirmed in the cell line selected for further analysis (#57). The antiproliferative action of PACAP in these cells was blocked by H89, a selective inhibitor of the cAMP-dependent protein kinase (PKA), indicating that PACAP action on these cells was probably mediated by the cAMP/PKA pathway. This is in line with our previous findings on PACAP/Shh interaction in cerebellar granule cell progenitors (Nicot et al., 2002), and reinforced the hypothesis that PACAP is an endogenous regulator of granular cell progenitors, and potentially plays a role in their transformation into MB, and/or on their rate of growth. We also measured the effect of PACAP on the Shh target gene *gli1* mRNA expression. PACAP also reduced *gli1* mRNA levels, an effect which was mimicked by forskolin, an inducer of cAMP production. A similar result was obtained using β -

galactosidase reporter gene assay as an alternative method to evaluate hedgehog pathway activity (data not shown). It would be interesting to know where PKA acts in the Hh signaling pathway in these cells. However this is difficult to study because it has been reported that the Hh pathway becomes significantly repressed when MB tumor cells from *ptc1* mutant mice are placed in culture, (Sasai et al., 2006). In agreement with that report, we found that proliferation and *gli1* gene expression were reduced by only 40–50% after treatment with the smoothed antagonist cyclopamine (data not shown). Thus, it remains uncertain where the PACAP/PKA and Hh pathways intersect in these cells.

The PACAP/*ptc1* DH mice generated here represent a unique new model for MB. Although combining *ptc1* mutations with *p53* mutations in mice results in an even higher incidence of MB tumors (Wetmore et al., 2001), the novelty of the PACAP/*ptc1* DH model is that the two targeted mutations appear to cooperate to derepress a common signaling pathway putatively involved in many human MBs, and to activate a number of other genes known to be overexpressed in human tumors. Moreover, the increased incidence of MB in *ptc1* +/- mice due to loss of PACAP suggests that a heterotrimeric G protein coupled receptor-mediated activation of PKA can antagonize a Hedgehog pathway-driven process. However, the experiments reported here do not rule out the possibility that that loss of PACAP enhanced tumors in *ptc1* mice due to a mechanism other than a reduction of PKA. PACAP is known to activate several other signaling pathways in parallel or downstream of cAMP, including pathways involving nitric oxide (Murthy et al., 1993), phospholipase C (Spengler et al., 1993), phosphatidylinositol 3-Kinase (Straub and Sharp, 1996), and src (Koh, 1991). In addition, in some cell types has been shown to act through MAP kinase pathways (Barrie et al., 1997; Lelievre et al., 1998; Villalba et al., 1997), inhibition of the NFkB cascade and Jak1/Jak2 phosphorylation (Delgado and Ganea, 1999; Delgado and Ganea, 2000).

In any case, the significance PACAP in the pathogenesis of human MB remains to be explored. Most human MB tumors in one series were found to express receptors which bind both PACAP and the closely-related peptide vasoactive intestinal peptide (Fruhwald et al., 1999). It is unknown if mutations in either PACAP or PACAP receptors are present in human MB tumors. With respect to the most common signaling pathway for PACAP (cAMP/PKA), a limited analysis of PKA genes showed no consistent LOH in a series of human MB tumors (Zurawel et al., 2000). However, PKA genes were not sequenced in this series, and other components of the cAMP signaling pathway, such as adenylate cyclases, and regulators of G protein signaling were not examined. The cAMP/PKA may also be important in modulating other signaling pathways in addition to Hh believed to be involved in the pathogenesis of MB. For example, several Wnt pathway genes have been implicated in medulloblastoma (reviewed in (Pietsch et al., 2004)). Different models systems indicate that PKA might act at several steps in this signaling pathway (Chen et al., 2005; Hino et al., 2005; Masai et al., 2005).

Finally, PACAP receptors are expressed on multiple types of cancer (Waschek et al., 2006). Although mutations in the genes encoding PACAP or any of its receptor subtypes have not yet been genetically linked to any of these malignancies, it may be of interest to determine the relevance of a PACAP/Hh interaction in the pathogenesis of the growing list of tumors that appear to involve overactive Hh signaling (Berman et al., 2003; Kaye et al., 2004; Kubo et al., 2004; Stecca et al., 2005; Thayer et al., 2003; Watkins et al., 2003).

Acknowledgements

This present work was supported by NIH grant CA110384, HD34475, and HD04612 (JW), CA121131 (LL), and the University of California at Los Angeles Neuro-Oncology Seed Grant Program, and Department of Energy Cooperative Agreement Contract number DE-FC03-02ER63420. VL is recipient of fellowship from INSERM/Fondation pour la Recherche Medicale (France).

References

- Aza-Blanc P, Ramirez-Weber FA, Laget MP, Schwartz C, Kornberg TB. Proteolysis that is inhibited by hedgehog targets Cubitus interruptus protein to the nucleus and converts it to a repressor. *Cell* 1997;89:1043–53. [PubMed: 9215627]
- Baillie GS, Scott JD, Houslay MD. Compartmentalisation of phosphodiesterases and protein kinase A: opposites attract. *FEBS Lett* 2005;579:3264–70. [PubMed: 15943971]
- Barrie AP, Clohessy AM, Buensuceso CS, Rogers MV, Allen JM. Pituitary adenylyl cyclase-activating peptide stimulates extracellular signal-regulated kinase 1 or 2 (ERK1/2) activity in a Ras-independent, mitogen-activated protein Kinase/ERK kinase 1 or 2-dependent manner in PC12 cells. *J Biol Chem* 1997;272:19666–71. [PubMed: 9242621]
- Berman DM, Karhadkar SS, Hallahan AR, Pritchard JI, Eberhart CG, Watkins DN, Chen JK, Cooper MK, Taipale J, Olson JM, Beachy PA. Medulloblastoma growth inhibition by hedgehog pathway blockade. *Science* 2002;297:1559–61. [PubMed: 12202832]
- Berman DM, Karhadkar SS, Maitra A, Montes De Oca R, Gerstenblith MR, Briggs K, Parker AR, Shimada Y, Eshleman JR, Watkins DN, Beachy PA. Widespread requirement for Hedgehog ligand stimulation in growth of digestive tract tumours. *Nature* 2003;425:846–51. [PubMed: 14520411]
- Chen AE, Ginty DD, Fan CM. Protein kinase A signalling via CREB controls myogenesis induced by Wnt proteins. *Nature* 2005;433:317–22. [PubMed: 15568017]
- Chen Y, Cardinaux JR, Goodman RH, Smolik SM. Mutants of cubitus interruptus that are independent of PKA regulation are independent of hedgehog signaling. *Development* 1999;126:3607–16. [PubMed: 10409506]
- Chomczynski P, Sacchi N. Single-step method of RNA isolation by acid guanidinium thiocyanate-phenol-chloroform extraction. *Anal Biochem* 1987;162:156–9. [PubMed: 2440339]
- Colwell CS, Michel S, Itri J, Rodriguez W, Tam J, Lelievre V, Hu Z, Waschek JA. Selective deficits in the circadian light response in mice lacking PACAP. *Am J Physiol Regul Integr Comp Physiol* 2004;287:R1194–201. [PubMed: 15217792]
- Corcoran RB, Scott MP. A mouse model for medulloblastoma and basal cell nevus syndrome. *J Neurooncol* 2001;53:307–18. [PubMed: 11718263]
- Delgado M, Ganea D. Vasoactive intestinal peptide and pituitary adenylate cyclase-activating polypeptide inhibit interleukin-12 transcription by regulating nuclear factor kappaB and Ets activation. *J Biol Chem* 1999;274:31930–40. [PubMed: 10542221]
- Delgado M, Ganea D. Inhibition of IFN-gamma-induced janus kinase-1-STAT1 activation in macrophages by vasoactive intestinal peptide and pituitary adenylate cyclase-activating polypeptide. *J Immunol* 2000;165:3051–7. [PubMed: 10975815]
- Ellison D. Classifying the medulloblastoma: insights from morphology and molecular genetics. *Neuropathol Appl Neurobiol* 2002;28:257–82. [PubMed: 12175339]
- Epstein DJ, Marti E, Scott MP, McMahon AP. Antagonizing cAMP-dependent protein kinase A in the dorsal CNS activates a conserved Sonic hedgehog signaling pathway. *Development* 1996;122:2885–94. [PubMed: 8787761]
- Fruhwald MC, O'Dorisio MS, Fleitz J, Pietsch T, Reubi JC. Vasoactive intestinal peptide (VIP) and VIP receptors: gene expression and growth modulation in medulloblastoma and other central primitive neuroectodermal tumors of childhood. *Int J Cancer* 1999;81:165–73. [PubMed: 10188714]
- Fukuda K, Yasugi S. Versatile roles for sonic hedgehog in gut development. *J Gastroenterol* 2002;37:239–46. [PubMed: 11993506]
- Goodrich LV, Milenkovic L, Higgins KM, Scott MP. Altered neural cell fates and medulloblastoma in mouse patched mutants. *Science* 1997;277:1109–13. [PubMed: 9262482]
- Gray SL, Cummings KJ, Jirik FR, Sherwood NM. Targeted disruption of the pituitary adenylate cyclase-activating polypeptide gene results in early postnatal death associated with dysfunction of lipid and carbohydrate metabolism. *Mol Endocrinol* 2001;15:1739–47. [PubMed: 11579206]
- Hammerschmidt M, Bitgood MJ, McMahon AP. Protein kinase A is a common negative regulator of Hedgehog signaling in the vertebrate embryo. *Genes Dev* 1996;10:647–58. [PubMed: 8598293]
- Hashimoto H, Shintani N, Tanaka K, Mori W, Hirose M, Matsuda T, Sakaue M, Miyazaki J, Niwa H, Tashiro F, Yamamoto K, Koga K, Tomimoto S, Kunugi A, Suetake S, Baba A. Altered psychomotor

- behaviors in mice lacking pituitary adenylyl cyclase-activating polypeptide (PACAP). *Proc Natl Acad Sci U S A* 2001;98:13355–60. [PubMed: 11687615]
- Hino S, Tanji C, Nakayama KI, Kikuchi A. Phosphorylation of beta-catenin by cyclic AMP-dependent protein kinase stabilizes beta-catenin through inhibition of its ubiquitination. *Mol Cell Biol* 2005;25:9063–72. [PubMed: 16199882]
- Jia J, Tong C, Wang B, Luo L, Jiang J. Hedgehog signalling activity of Smoothened requires phosphorylation by protein kinase A and casein kinase I. *Nature* 2004;432:1045–50. [PubMed: 15616566]
- Kayed H, Kleeff J, Keleg S, Guo J, Ketterer K, Berberat PO, Giese N, Esposito I, Giese T, Buchler MW, Friess H. Indian hedgehog signaling pathway: expression and regulation in pancreatic cancer. *Int J Cancer* 2004;110:668–76. [PubMed: 15146555]
- Kenney AM, Cole MD, Rowitch DH. Nmyc upregulation by sonic hedgehog signaling promotes proliferation in developing cerebellar granule neuron precursors. *Development* 2003;130:15–28. [PubMed: 12441288]
- Kimura H, Kawatani M, Ito E, Ishikawa K. Effects of pituitary adenylyl cyclase-activating polypeptide on facial nerve recovery in the Guinea pig. *Laryngoscope* 2003;113:1000–6. [PubMed: 12782812]
- Kimura H, Stephen D, Joyner A, Curran T. Gli1 is important for medulloblastoma formation in Ptc1+/- mice. *Oncogene* 2005;24:4026–36. [PubMed: 15806168]
- Kleihues, P.; Cavenee, WK. International Agency for Research on Cancer., and International Society of Neuropathology. Pathology and genetics of tumours of the nervous system; International Agency for Research on Cancer, Lyon. 1998.
- Koh SW. Signal transduction through the vasoactive intestinal peptide receptor stimulates phosphorylation of the tyrosine kinase pp60c-src. *Biochem Biophys Res Commun* 1991;174:452–8. [PubMed: 1704221]
- Kubo M, Nakamura M, Tasaki A, Yamanaka N, Nakashima H, Nomura M, Kuroki S, Katano M. Hedgehog signaling pathway is a new therapeutic target for patients with breast cancer. *Cancer Res* 2004;64:6071–4. [PubMed: 15342389]
- Lelievre V, Caigneaux E, Muller JM, Falcon J. Extracellular adenosine deprivation induces epithelial differentiation of HT29 cells: evidence for a concomitant adenosine A(1)/A(2) receptor balance regulation. *Eur J Pharmacol* 2000;391:21–9. [PubMed: 10720631]
- Lelievre V, Pineau N, Du J, Wen CH, Nguyen T, Janet T, Muller JM, Waschek JA. Differential effects of peptide histidine isoleucine (PHI) and related peptides on stimulation and suppression of neuroblastoma cell proliferation. A novel VIP-independent action of PHI via MAP kinase. *J Biol Chem* 1998;273:19685–90. [PubMed: 9677397]
- Leung C, Lingbeek M, Shakhova O, Liu J, Tanger E, Saremaslani P, Van Lohuizen M, Marino S. Bmi1 is essential for cerebellar development and is overexpressed in human medulloblastomas. *Nature* 2004;428:337–41. [PubMed: 15029199]
- Li W, Ohlmeyer JT, Lane ME, Kalderon D. Function of protein kinase A in hedgehog signal transduction and Drosophila imaginal disc development. *Cell* 1995;80:553–62. [PubMed: 7867063]
- Lum L, Beachy PA. The Hedgehog response network: sensors, switches, and routers. *Science* 2004;304:1755–9. [PubMed: 15205520]
- Masai I, Yamaguchi M, Tonou-Fujimori N, Komori A, Okamoto H. The hedgehog-PKA pathway regulates two distinct steps of the differentiation of retinal ganglion cells: the cell-cycle exit of retinoblasts and their neuronal maturation. *Development* 2005;132:1539–53. [PubMed: 15728672]
- Murthy KS, Zhang KM, Jin JG, Grider JR, Makhlof GM. VIP-mediated G protein-coupled Ca²⁺ influx activates a constitutive NOS in dispersed gastric muscle cells. *Am J Physiol* 1993;265:G660–71. [PubMed: 7694477]
- Nicot A, Lelievre V, Tam J, Waschek JA, DiCicco-Bloom E. Pituitary adenylyl cyclase-activating polypeptide and sonic hedgehog interact to control cerebellar granule precursor cell proliferation. *J Neurosci* 2002;22:9244–54. [PubMed: 12417650]
- Nielsen HS, Hannibal J, Fahrenkrug J. Expression of pituitary adenylyl cyclase activating polypeptide (PACAP) in the postnatal and adult rat cerebellar cortex. *Neuroreport* 1998;9:2639–42. [PubMed: 9721947]

- Pietsch T, Taylor MD, Rutka JT. Molecular pathogenesis of childhood brain tumors. *J Neurooncol* 2004;70:203–15. [PubMed: 15674478]
- Poh A, Karunaratne A, Kolle G, Huang N, Smith E, Starkey J, Wen D, Wilson I, Yamada T, Hargrave M. Patterning of the vertebrate ventral spinal cord. *Int J Dev Biol* 2002;46:597–608. [PubMed: 12141448]
- Reifenberger J, Wolter M, Weber RG, Megahed M, Ruzicka T, Lichter P, Reifenberger G. Missense mutations in SMOH in sporadic basal cell carcinomas of the skin and primitive neuroectodermal tumors of the central nervous system. *Cancer Res* 1998;58:1798–803. [PubMed: 9581815]
- Sasai K, Romer JT, Lee Y, Finkelstein D, Fuller C, McKinnon PJ, Curran T. Shh pathway activity is down-regulated in cultured medulloblastoma cells: implications for preclinical studies. *Cancer Res* 2006;66:4215–22. [PubMed: 16618744]
- Spengler D, Waeber C, Pantaloni C, Holsboer F, Bockaert J, Seeburg PH, Journot L. Differential signal transduction by five splice variants of the PACAP receptor. *Nature* 1993;365:170–5. [PubMed: 8396727]
- Stecca B, Mas C, Ruiz i Altaba A. Interference with HH-GLI signaling inhibits prostate cancer. *Trends Mol Med* 2005;11:199–203. [PubMed: 15882606]
- Straub SG, Sharp GW. A wortmannin-sensitive signal transduction pathway is involved in the stimulation of insulin release by vasoactive intestinal polypeptide and pituitary adenylate cyclase-activating polypeptide. *J Biol Chem* 1996;271:1660–8. [PubMed: 8576167]
- Tao Y, Black IB, DiCicco-Bloom E. In vivo neurogenesis is inhibited by neutralizing antibodies to basic fibroblast growth factor. *J Neurobiol* 1997;33:289–96. [PubMed: 9298766]
- Thayer SP, di Magliano MP, Heiser PW, Nielsen CM, Roberts DJ, Lauwers GY, Qi YP, Gysin S, Fernandez-del Castillo C, Yajnik V, Antoniu B, McMahon M, Warshaw AL, Hebrok M. Hedgehog is an early and late mediator of pancreatic cancer tumorigenesis. *Nature* 2003;425:851–6. [PubMed: 14520413]
- Tiecke E, Turner R, Sanz-Ezquerro JJ, Warner A, Tickle C. Manipulations of PKA in chick limb development reveal roles in digit patterning including a positive role in Sonic Hedgehog signaling. *Dev Biol* 2007;305:312–24. [PubMed: 17376427]
- Vaudry D, Gonzalez BJ, Basille M, Yon L, Fournier A, Vaudry H. Pituitary adenylate cyclase-activating polypeptide and its receptors: from structure to functions. *Pharmacol Rev* 2000;52:269–324. [PubMed: 10835102]
- Villalba M, Bockaert J, Journot L. Pituitary adenylate cyclase-activating polypeptide (PACAP-38) protects cerebellar granule neurons from apoptosis by activating the mitogen-activated protein kinase (MAP kinase) pathway. *J Neurosci* 1997;17:83–90. [PubMed: 8987738]
- Waschek JA. Multiple actions of pituitary adenylyl cyclase activating peptide in nervous system development and regeneration. *Dev Neurosci* 2002;24:14–23. [PubMed: 12145407]
- Waschek JA, Casillas RA, Nguyen TB, DiCicco-Bloom EM, Carpenter EM, Rodriguez WI. Neural tube expression of pituitary adenylate cyclase-activating peptide (PACAP) and receptor: potential role in patterning and neurogenesis. *Proc Natl Acad Sci U S A* 1998;95:9602–7. [PubMed: 9689127]
- Waschek JA, DiCicco-Bloom E, Nicot A, Lelievre V. Hedgehog signaling: new targets for GPCRs coupled to cAMP and protein kinase A. *Ann N Y Acad Sci* 2006;1070:120–8. [PubMed: 16888153]
- Watkins DN, Berman DM, Burkholder SG, Wang B, Beachy PA, Baylin SB. Hedgehog signalling within airway epithelial progenitors and in small-cell lung cancer. *Nature* 2003;422:313–7. [PubMed: 12629553]
- Wechsler-Reya RJ, Scott MP. Control of neuronal precursor proliferation in the cerebellum by Sonic Hedgehog. *Neuron* 1999;22:103–14. [PubMed: 10027293]
- Wetmore C, Eberhart DE, Curran T. The normal patched allele is expressed in medulloblastomas from mice with heterozygous germ-line mutation of patched. *Cancer Res* 2000;60:2239–46. [PubMed: 10786690]
- Wetmore C, Eberhart DE, Curran T. Loss of p53 but not ARF accelerates medulloblastoma in mice heterozygous for patched. *Cancer Res* 2001;61:513–6. [PubMed: 11212243]
- Yokota N, Mainprize TG, Taylor MD, Kohata T, Loreto M, Ueda S, Dura W, Grajkowska W, Kuo JS, Rutka JT. Identification of differentially expressed and developmentally regulated genes in

medulloblastoma using suppression subtraction hybridization. *Oncogene* 2004;23:3444–53.
[PubMed: 15064731]

Zurawel RH, Allen C, Chiappa S, Cato W, Biegel J, Cogen P, de Sauvage F, Raffel C. Analysis of PTCH/
SMO/SHH pathway genes in medulloblastoma. *Genes Chromosomes Cancer* 2000;27:44–51.
[PubMed: 10564585]

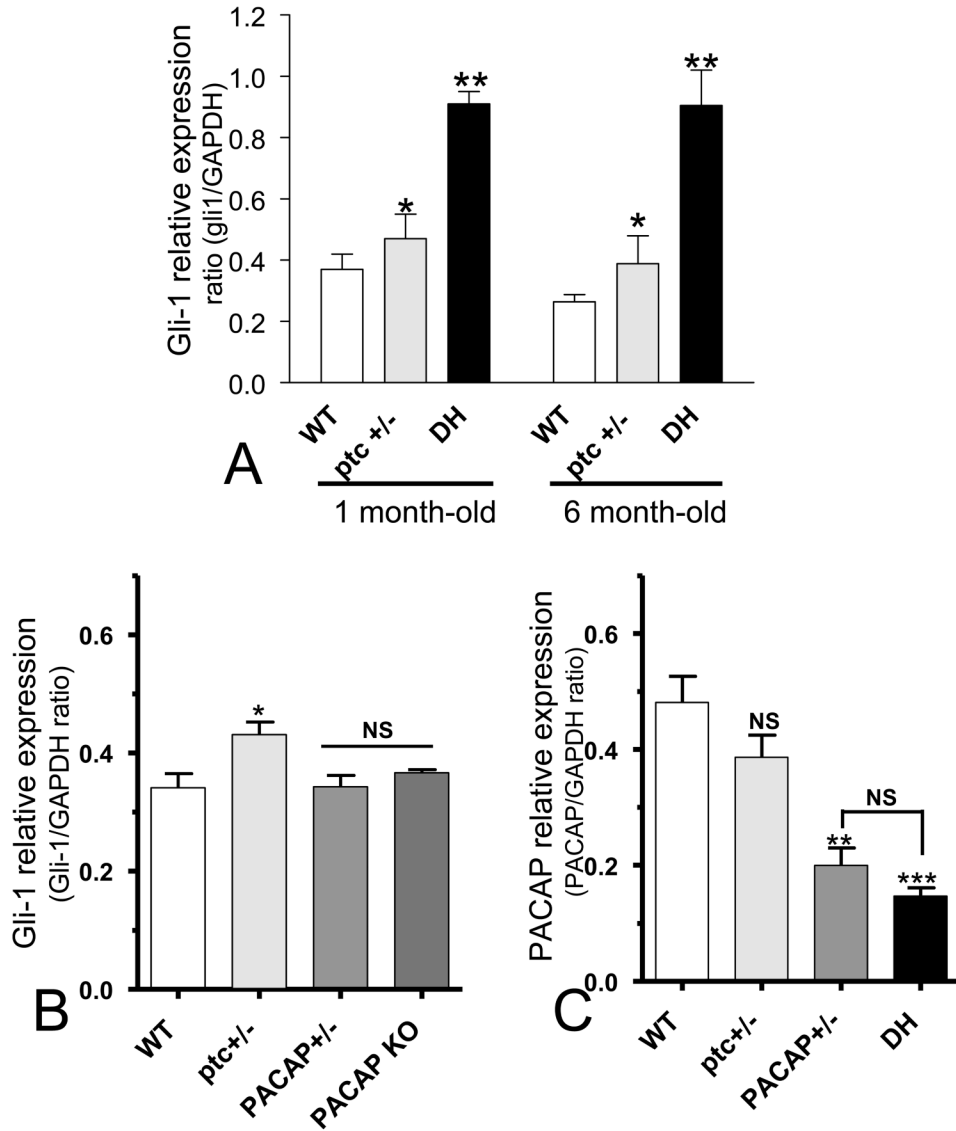


Figure 1. *Gli1* and PACAP gene expression in isolated cerebella from wild-type (WT), *ptc1*^{+/-}, PACAP^{+/-}, PACAP KO or *ptc1*/PACAP double mutant (DH) mice

A: Comparison of *gli1* gene expression (as determined by quantitative real time RT-PCR) in cerebella from WT one and six-month old wild type, *ptc1*^{+/-} and DH mice. Cerebella were dissected and examined under the stereomicroscope to exclude animals harboring obvious cerebellar abnormalities. Cerebella from *ptc1*^{+/-} mice and PACAP/*ptc1* DH exhibited significantly higher *gli1* gene expression than WT. Cerebella from DH mice exhibited significantly higher expression than those from *ptc1*^{+/-} mice. **B:** *Gli1* gene expression levels in cerebella from 1 month-old WT, PACAP^{+/-} PACAP^{-/-} and *ptc1* mutants showed no direct effect of PACAP gene disruption alone on Shh target gene expression. **C:** PACAP gene expression in WT, *ptc1* and PACAP mutants showed no effect of *ptc1* mutation on PACAP gene expression. Values are mean \pm SEM (n= 7 per group); *p \leq 0.05; **p<0.01 (ANOVA).

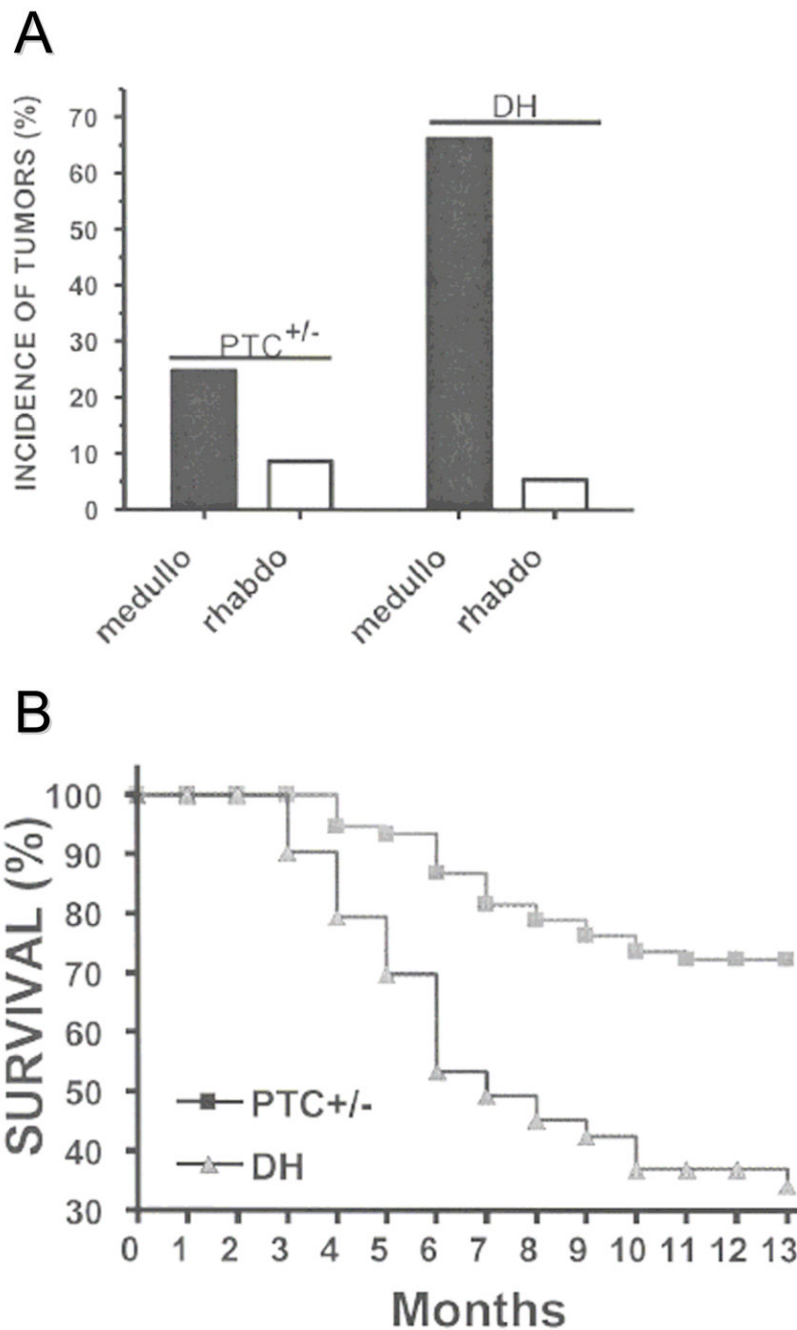


Figure 2. Effect of PACAP gene disruption on the incidence of MB in *ptc1* mutants over 1 year
A: Overall comparison between *ptc1*^{+/-} and *ptc1*/PACAP double heterozygous (DH) mutants revealed a 2.5-fold increase in medulloblastoma in the latter group. 77 and 73 mice were in the *ptc1*^{+/-} and DH group, respectively. Statistical analysis using the chi2 contingency test revealed significant differences between *ptc1* and DH groups at p=.019. **B:** Survival from medulloblastoma in *ptc1*^{+/-} animals vs. DH mutants. Double mutants exhibit an overall six week-earlier mean age of death from medulloblastoma than *ptc1*^{+/-} animals. The survival curves were created using the product limit method of Kaplan and Meier (Prism4, Graphpad™) and comparison of survival curves between *ptc1* and DH mutants was performed using the logrank test. Analysis revealed statistical differences at P<0.0001.

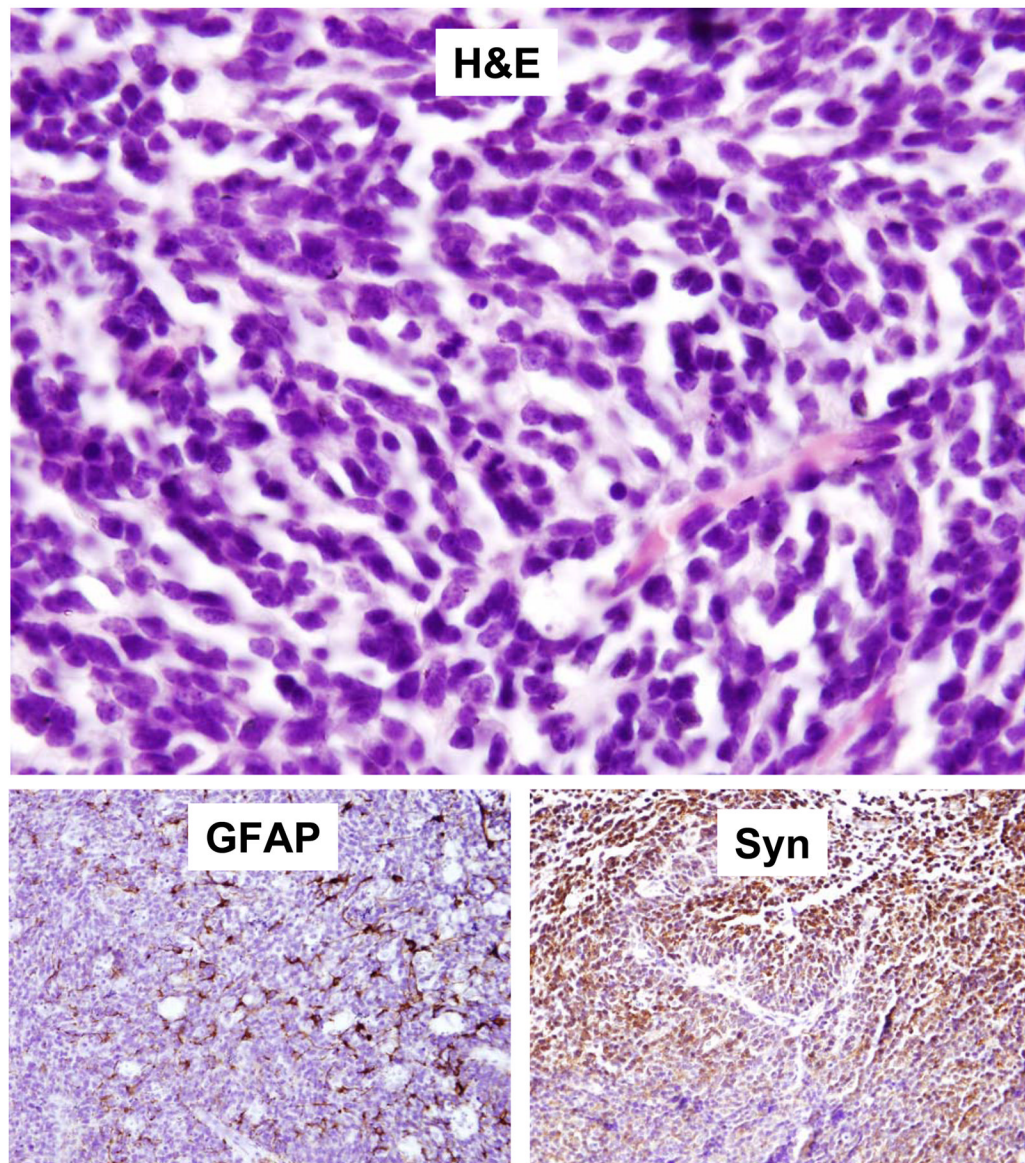


Figure 3. Histological characteristics, synaptophysin and GFAP immunoreactivities in representative tumors arising in *ptc1*/PACAP mutant mice
Top panel shows section of tumor from a *ptc1*/PACAP double mutant mouse stained with hematoxylin/eosin (H&E). Bottom panels show sections stained with antibodies for synaptophysin (Syn) (left) and GFAP (right).

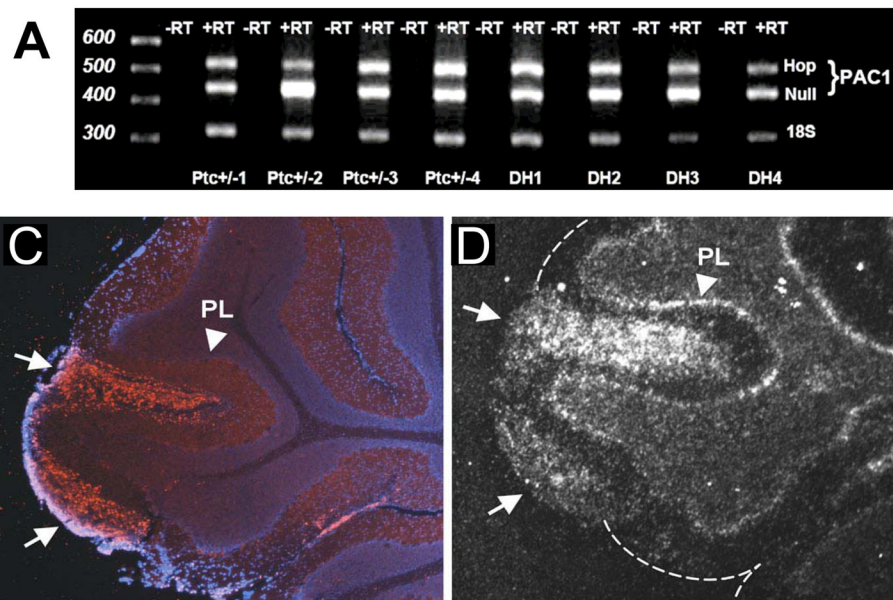


Figure 4. PACAP receptor (PAC1) gene expression in representative tumors and in an ectopic patch of proliferating EGL. Panel A

demonstrates PACAP receptor PAC₁ gene expression in selected tumors from *ptc1* and PACAP/*ptc1* double heterozygous mice, determined by RT-PCR. The two bands correspond to the “hop” and “null” forms of PAC₁ mRNAs which putatively can couple the receptor to other signal transduction pathways, including PLC and MAP kinase in addition to PKA (Spengler et al., 1993). Genotype is indicated at bottom. **Panel B:** Ki-67 fluorescent immunohistochemistry shows a hyperplastic region of proliferating cells on the surface of the cerebellum of a postnatal day 28 DH mouse. Section is counterstained with DAPI. **Panel C:** ³³P *in situ* hybridization and dark field illumination that demonstrates that PACAP receptor (PAC1) gene transcripts are abundant in the hyperplastic lesion. Ectopic hyperplastic region is indicated with arrows. PL= Purkinje layer. PAC1 receptors are abundant in the ectopic lesion. In addition, PAC1 gene expression is present in the Purkinje layer, and at low levels in the internal granular

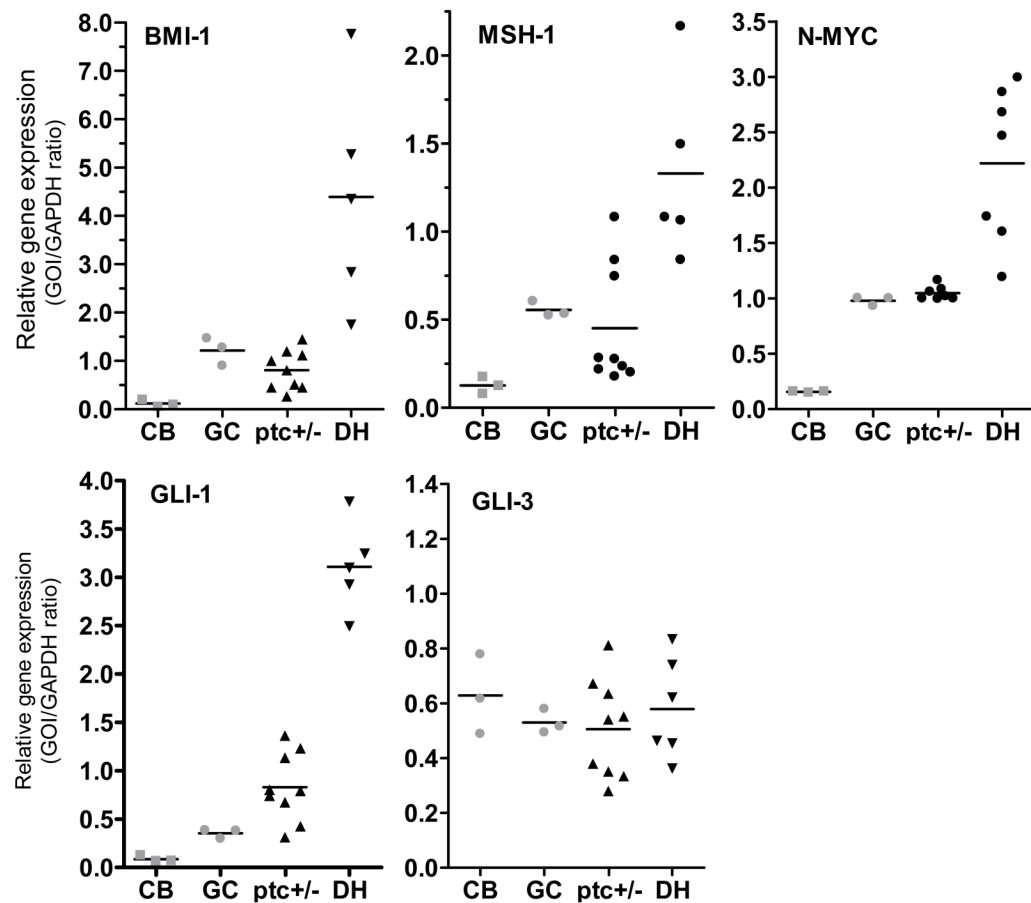


Figure 5. Gene expression in freshly-resected MB tumors from *ptc1*^{+/-} vs. DH mice

Comparison of expression of several genes in tumors from *ptc1*^{+/-} vs. DH mice by real time RT-PCR. Tumor samples from DH mice showed significant increases in *BMI1*, *MSH1*, *gli1*, and *Nmyc*, when compared to tumors isolated from *ptc1* mutants (ANOVA, $p < 0.01$) or from wild-type C57BL/6J total cerebellum or isolated granular cell progenitors. Conversely, no differences were observed between groups when amplification was done with *gli3* primer sets. Values are expressed relative to the control gene GAPDH. The increased expressions of *Gli1*, and *BMI* were confirmed using $\beta 2$ -microglobulin mRNA as an alternative housekeeping mRNA control. Mean values are indicate with a horizontal line. Statistical analyses were performed using one way-ANOVA followed by pairwise comparison using Bonferroni ad-hoc post-test when overall $p < 0.05$. GOI = gene of interest; CB = adult cerebellum, GC = cerebellar granule cells freshly isolated from postnatal day 6 mice as described in the methods section.

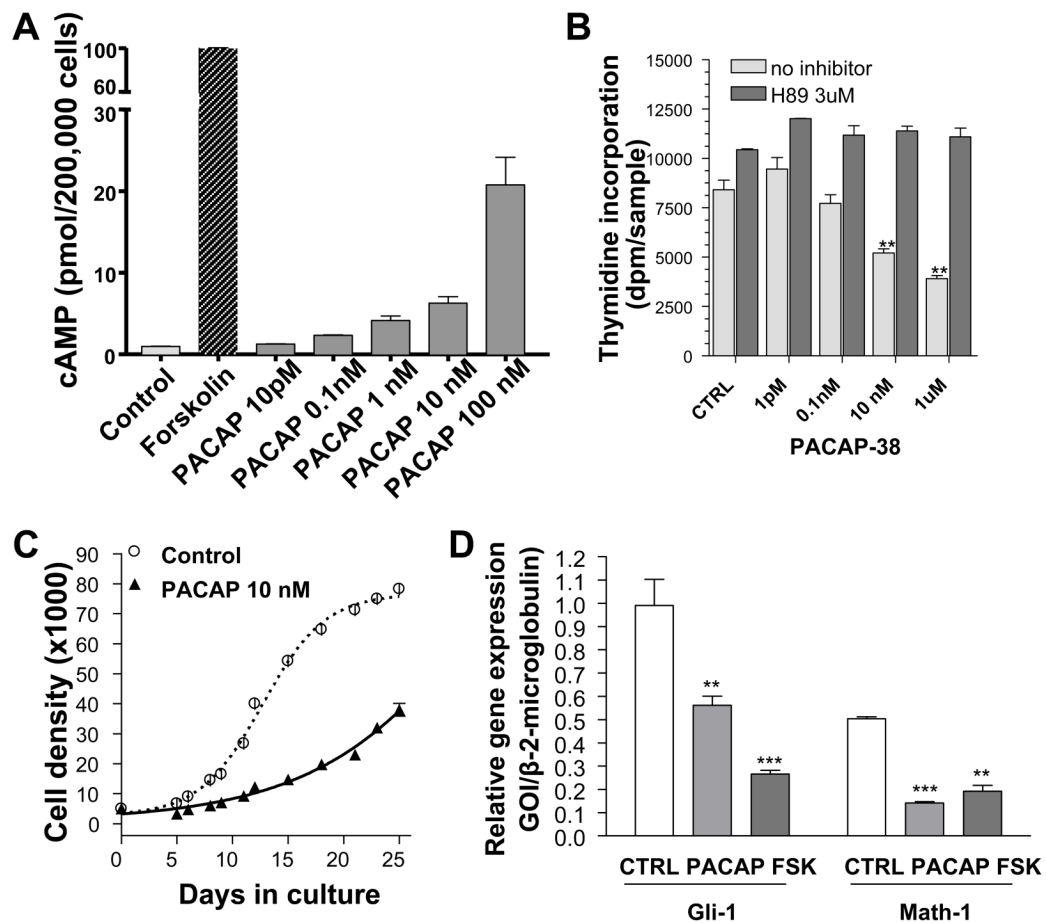


Figure 6. Action of PACAP and Shh on proliferation and *gli1* gene expression in MB cell line #57
A: cAMP induction by forskolin 1 μ M and by increasing concentrations of PACAP. **B:** Concentration-dependent antiproliferative action of PACAP-38 and blockade by 3 μ M of the PKA antagonist H89. Cells were treated for six hours. **C:** Long-term reduction in cell proliferation by daily addition of 10 nM PACAP. **D:** Reduction in gene expression of *gli1* and *Math1* induced by 12 hr treatment with 10 nM PACAP or 20 μ M forskolin. For panels B–D, three independent experiments were performed in triplicate. Results were consistent between experiments, and representative data are shown. Statistical analyses in B and D were performed with one way-ANOVA followed by pairwise comparison using Bonferroni ad-hoc post-test (performed when overall $p < 0.05$); Significant differences at $p < *0.05$, $**0.01$ or $***0.005$. Statistical analysis of data in panel C using ANOVA followed by Bonferroni ad hoc post test showed that significant differences ($p < 0.001$)

Table 1**Genotypes of 130 mice derived from interbreedings of PACAP/*ptc1* double heterozygous mice**

Genotyping was performed 6 weeks after birth.

		PACAP genotype		
		+/+	+/-	-/-
<i>ptc1</i>	+/+	14	27	1
genotype	+/-	33	52	1*
	-/-	0	0	0

* This mouse died of unknown causes within one week of DNA sampling

Table 2

PACAP inhibition of DNA synthesis in several cell lines established from medulloblastoma tumors arising in *ptc1* +/- and mice mice double heterozygous (DH) for *ptc1* +/- and PACAP.

Cell line	Genotype	Proliferation (% of control)
961	<i>ptc1</i> +/-	80 +/-1.7*
1393	<i>ptc1</i> +/-	93 +/-4.2§
1395	<i>ptc1</i> +/-	74 +/-6.2**
1713	<i>ptc1</i> +/-	56 +/-2.6**
1717	<i>ptc1</i> +/-	48 +/-6.2**
57	DH	68 +/-3.5**

Statistically analyzed by ANOVA:

* p<0.05*,

** p<001,

§ not significant.